Journal of Magnetism and Magnetic Materials 323 (2011) 410–415

Contents lists available at ScienceDirect

Journal of Magnetism and Magnetic Materials

journal homepage: www.elsevier.com/locate/jmmm

An original route to stabilize and functionalize magnetite nanoparticles for theranosis applications

D. Forge [a], S. Laurent [a], Y. Gossuin [b], A. Roch [a], L. Vander Elst [a], R.N. Muller [a,*]

[a] Department of General, Organic and Biomedical Chemistry, NMR and Molecular Imaging Laboratory, University of Mons, 24 Avenue du Champ de Mars, B-7000 Mons, Belgium
[b] Biological Physics Department, University of Mons, 24 Avenue du Champ de Mars, B-7000 Mons, Belgium

ARTICLE INFO

Article history:
Received 11 May 2010
Received in revised form
17 September 2010
Available online 16 October 2010

Keywords:
Monodisperse magnetic fluid
Colloïdal stability
Biomedical application
Silane coupling agent
Magnetic filtration

ABSTRACT

A versatile method for the introduction of cyano groups onto the surface of iron oxide nanoparticles has been developed. This protocol is based on the hydrolysis and the condensation of cyanoethyltrimethoxysilane (CES) on the magnetite surface. The optimal concentration of silane coupling agent was determined ([Fe]/[CN] ratio = 0.4) in order to obtain an appropriate surface density of activating groups on the nanoparticles. The size distribution of the particles was also optimized by a magnetic size sorting procedure. An adequate surface with cyano groups could facilitates their use in biomedical applications by improving the cellular labeling and the cell targeting.

1. Introduction

The stabilization of iron oxide particles is crucial in order to obtain magnetic colloidal ferrofluids that do not aggregate in a biological medium and/or in a magnetic field. Such modified magnetic nanoparticles have indeed an important role in biomedical applications [1–4] such as magnetic resonance molecular imaging (MRMI), hyperthermia, drug delivery, cellular labeling or protein separation. All of these applications require nanoparticles with high saturation magnetization, a narrow size distribution and a peculiar surface coating. It is thus necessary to develop an efficient strategy to improve the chemical stability, the functionnalization and the size dispersion of magnetite nanoparticles.

Chemical stability is related to the balance between attractive and repulsive forces acting between the particles [5]. The theoretical description of these two forces is known as the Derjarguin–Landau–Verwey–Overbeek (DLVO) theory [6]. In order to prevent the aggregation of particles, a repulsive force between them may be created through sterical or electrostatic repulsions produced by a core-shell structure. Such modified magnetic nanoparticles are composed of one iron oxide core coated with organic or inorganic molecules, which are responsible for the repulsive forces between particles. Several types of steric (PEG, dextran, PAA, PVA, etc.) or electrostatic (carboxylates, silica, gold, phosphates, etc.) coatings have been reported in the literature [7–9]. However, for *in vivo* applications, the biocompatibility, the toxicity and the biodegradation properties have to be considered for the choice of the magnetic structure. Numerous studies reveal a relationship between physicochemical parameters of ferrofluids and their toxicity [10,11]. In general, iron oxide nanoparticles have a good biocompatibility profile [12]. However, depending on the shape of the nanoparticles [13], it can be reduced by cell interaction with nanobeads, nanoworms and nanosphere. Other important factors that determine the toxicity of nanoparticles are the surface charge, surface area, oxidation and size [14,15]. When compared to micron-sized particles, it is generally accepted that nano-sized particle can be more toxic because they have a larger surface area to interact with cell membranes. Moreover, their surface characteristics are important since they seem to be the determining factor for cell uptake and cytotoxicity. The coating of the particles has to be non cytotoxic. The shell must also have active groups, which can be conjugated to biomolecules such as thiols or amino functions. In this context, surface coating of iron oxide using organosilanes is really promising.

Organosilanes are bifunctional molecules with the general formula $X\text{-}(CH_2)_n\text{-}Si(OR)_n$ where X represents the headgroup functionality, $(CH_2)_n$ a flexible spacer, and $Si(OR)_n$ the anchor groups on free Fe-OH surface groups. Surface modification with organosilanes is an attractive approach because of their commercial availability as well as the large variety of functionalities. The silane coupling allows direct covalent bonds with bioligands through the organofunctionalities. (3-Aminopropyl)trimethoxysilane (APS; $NH_2(CH_2)_3Si(OCH_3)_3$) is the organosilane most frequently found in the literature [16–19]. Its active NH_2 group is able to combine with biomolecules, drugs, etc.

In this work we report an original preparation of superparamagnetic magnetite particles coated with cyanoethyltrimethoxysilane (CES; $CN(CH_2)_2Si(OCH_3)_3$). This coupling agent also offers interesting

* Corresponding author. Tel./fax: +32 65 373520.
E-mail address: robert.muller@umons.ac.be (R.N. Muller).

0304-8853/$ - see front matter © 2010 Elsevier B.V. All rights reserved.
doi:10.1016/j.jmmm.2010.09.031

prospects for grafting biomolecules (antibodies, peptides, proteins) via the cyano group [20,21], which will ease their use for molecular imaging applications. Indeed, an original way of covalent grafting is to use the click-chemistry principle to immobilize peptides on the surface of the particles. Briefly, click-chemistry is a recent concept, developed by Sharpless [22], which allows generating original and different structures via carbon–heteroatom bonds. In our case, the cycloaddition of an azide peptide on the cyanoferrofluid could lead to the formation of a covalent bond between the ferrofluid surface and the targeting agent in aqueous solution. Cellular magnetic labeling is an important tool for biomedical research, allowing for a non-invasive visualization of cells by MRI [23]. The cellular uptake of iron oxide nanoparticles is often optimized by combining the superparamagnetic contrast media with transfection agents in order to form complexes with a net positive charge. These complexes can thus be adsorbed on the negatively charged cell surface, initiating the endocytosis of the magnetic tag. However, high concentrations of these agents are toxic [24]. Negatively charged coatings have also been used to improve the magnetic labeling of cells. Indeed, it was hypothesized that the anionic coating allowed initiation of an adsorptive endocytosis mechanism, by strongly and nonspecifically binding on cationic sites of the plasma membrane. The presence of the negative charges of cyanoferrofluid synthesized in this work can consequently improve magnetic labeling efficiency at physiological pH.

The process of surface modification by the silanization reaction is complex [25–27]. Experimental parameters such as reaction temperature, silane concentration, pH, solvent nature, etc. can influence the reactivity of the silane molecule with the inorganic surface. In a simplified scheme, the reaction between an alkoxysilane and iron oxide nanoparticles involves a two-step reaction. The first step is the hydrolysis of alkoxide groups $-OCH_3$ to the highly reactive silanol species; and the second step is the condensation of the silanol groups with the free Fe-OH groups of the iron oxide surface.

Our strategy is to adapt the experimental protocol developed by Duguet et al. [28] to the cationic ferrofluids synthesized previously, in order to obtain an optimal covering on the magnetite surface.

Moreover, the size distribution of the particles is a very important characteristic of these materials since it influences their colloidal stability and their efficiency for these biomedical applications. For example, the characteristics of smaller particles such as Ultra Small Super Paramagnetic Iron Oxide (USPIO) open up new clinical applications in MRI [29] like the targeting of organs other than those belonging to the reticuloendothelial system (RES). Thus, a magnetic size sorting procedure developed previously [30] has also been used in this work to narrow the size distribution of the cyanoferrofluid.

In summary, this article describes the preparation of the cationic ferrofluids, their surface modification with cyano functions, and the optimization of their size dispersion.

2. Experimental methods

2.1. Materials

Cyanoethyltrimethoxysilane (CES) and (3-aminopropyl)trimethoxysilane (APS) were purchased from ABCR GmbH & Co. KG (Karlsruhe, Germany). All others reagents used were obtained from Aldrich (Bornem, Belgium) and were of the highest purity grade.

2.2. Formation of stabilized ferrofluids

2.2.1. Formation of magnetite nanoparticles

This protocol includes the formation of γ-Fe_2O_3 nanoparticles in organic medium, whereas their dispersion is performed in aqueous medium. The levels of the co-precipitation parameters were optimized previously by the design of experiments method [31]. Briefly, a 25 ml equimolar mixture of $FeCl_2$ and $FeCl_3$ (3.3 M with $[Fe^{2+}]/[Fe^{3+}]=1$) in diethyleneglycol (250 ml) was heated at 170 °C. After 10 min, solid (pellet) NaOH (15 g) was added in order to prevent the addition of any aqueous media. The solution was stirred during 1 h at 170 °C. This mixture was then cooled to room temperature. The black gelatinous precipitate was isolated from the solution by magnetic decantation ($B_0=0.5$ T). This precipitate was then washed five times with an aqueous solution of nitric acid (125 ml, 1 M). Finally, the precipitate was dispersed in deionized water and centrifuged at 10,000 rpm for 15 min to remove aggregates.

2.2.2. Surface silanization of magnetite nanoparticles

For the silanization reaction of the magnetite nanoparticles, a modification of Duguet's method was used [28]. A solution of methanol and CES (10 ml) was added dropwise for 5 min to a suspension of protoned ferrofluid (20 ml, 0.25 M) dispersed into 10 ml of methanol. After stirring at room temperature for 12 h, 20 ml of glycerol were added. Then, methanol and water were removed at 40 and 80 °C for methanol and for 2 h at 100 °C for water. Flocculated CES-modified nanoparticles were washed three times with 40 ml of acetone. Following the addition of 40 ml of water, peptization was performed by slowly increasing pH from 3 to 10 with sodium hydroxide under vigorous stirring.

The importance of this procedure for this study is to modify the [Fe]/[CN] ratio in order to find the optimal density coating on the iron particle surface.

2.3. Characterization of nanoparticles

The size of nanoparticles can be evaluated by various techniques. The values of the crystal radius (r) and the saturation magnetization (M_S) [32] were first determined by the fitting of the magnetometric profiles (VSM-NUOVO MOLSPIN/ Newcastle upon Tyne, UK) using a Langevin function (Eq. (1)).

$$M = M_{sat}L(\alpha) \tag{1}$$

where $L(\alpha)=\coth(\alpha)-(1/\alpha)$ is the Langevin function and $\alpha=(\mu B_0/k_BT)$ with μ being the magnetic moment of the particle, k_B the Boltzmann constant and T the absolute temperature.

An additional way to determine r and M_S is the fitting of the proton nuclear magnetic relaxation rate profile recorded over a wide range of magnetic fields [33]. These Nuclear Magnetic Relaxation Dispersion (NMRD) profiles were recorded with a field cycling relaxometer (STELAR, Mede, Italy) measuring the longitudinal relaxation rates (R_1) in a magnetic field range extending from 0.24 mT to 0.24 T. The temperature of the samples was adjusted to 37 °C with a precision of 0.1 °C. Additional longitudinal (R_1) and transverse (R_2) relaxation rate measurements at 0.47 and 1.41 T were, respectively, obtained on Minispec MQ 20 and MQ 60 spin analyzers (Bruker, Karlsruhe, Germany).

Finally, the size and the shape of the particles were also investigated by transmission electron microscopy (TEM; CM 20, Philips, USA). The hydrodynamic sizes (d_H) and the surface charge were obtained with a Zêtasizer Nanoseries ZEN 3600 (MALVERN, United Kingdom). This size is an intensity-weighted mean value. A correct conversion to a number or volume-weighted mean value requires the knowledge of the complex refractive index.

The total iron concentration was determined by the measuring the longitudinal relaxation rate R_1 according to the method previously described [34]. Briefly, the samples were mineralized by microwave digestion in acidic and oxidant conditions (MLS-1200 MEGA, MILESTONE, Analis, Namur, Belgium). The R_1 value of the resulting solutions was recorded at 0.47 T and 37 °C, which

allowed determining iron concentration, using the following equation:

$$[Fe] = (R_1^{sample} - R_1^{diam})0.0915 \quad (2)$$

where R_1^{diam} (s^{-1}) is the diamagnetic relaxation rate of acidified water (0.36 s^{-1}) and 0.0915 (s mM) is the slope of the calibration curve.

The organic coating present on the particle's surface was determined by Time of flight secondary ion mass spectrometry (TOF-SIMS) measurements (TOF-SIMS 4, Ion Tof, Münster, Germany).

2.4. Magnetic filtration

The magnetic sorting was carried with magnetic separation columns (Miltenyi Biotec BU, Utrecht, The Netherlands, LS column MACS). When placed in an electromagnet, the MACS column matrix creates strong magnetic field gradients retaining magnetic particles according to their global magnetic moments and hence to their sizes. For each size sorting, 5 ml of 50 mM cyanoferrofluid (corresponding to about 10^{15} particles) are put into the column. The separation is essentially gravitational; there is no elution flow control. In this work, we characterized the particles that were not retained in the column. The magnetic fields used for this separation ranged from 250 to 2000 G.

3. Results and discussion

3.1. Determination of the optimal [Fe]/[CN] ratio

The initial magnetite ferrofluid was prepared in a large scale and reproducible manner according to a modified Massart's method [35]. In such conditions, the mean hydrodynamic diameter of the nanoparticles is 25 nm and the mean radius of the magnetic crystal, evaluated by relaxometry, is 5.7 nm (Table 1).

The colloïdal stability of these magnetic dispersions has to be ensured by electrostatic repulsions. We found, however, that at physiological pH (pH = 7.3), the electrostatic repulsions are very weak (zeta potential value = −0.9 mV). At this pH, the weaker electrostatic repulsion forces compared to the Van Der Waals attractive forces cause the destabilization of the ferrofluid, thus limiting biomedical applications. The goal of the coating process with cyanoethyltrimethoxysilane (CES) is the transition of the colloïdal stability control from electrostatic repulsions to steric ones by shifting the Point of Zero Charge (PZC) of the magnetite.

To ensure an effective stabilization of the cationic ferrofluids, several tests were carried out by modifying the ratio between the concentrations of the cationic ferrofluid and the CES. Generally, this ratio, noted [Fe]/[CN], ranges between 0.1 and 0.8.

The grafting of the CES on the iron oxide nanoparticles modifies the physicochemical properties of their surface. These modifications are reflected by the state of ionization of the functionalized ferrofluids according to the pH. Fig. 1 shows the zeta potential variations of cyanoferrofluid according to the concentration of CES and the pH. The PZC was found at pH 7.2 for the cationic magnetite ferrofluid. After silanization, the PZC was found at pH 3 thanks to the CES coating. Weak concentrations of CES are enough to modify the PZC of the magnetite. At pH > 3, the iron oxide particles' surface is negatively charged. Similar results [36] were previously explained on the basis of hydrolysis of the cyano functions in cationic medium and basic medium. The PZC being similar to that of the nanoparticles covered with silica [37], another possible explanation would be the protonation or deprotonation of the residual silanol functions present at the particle's surface.

Table 1 shows the relaxometric characteristics of these ferrofluids with an [Fe]/[CN] ratio ranging between 0.1 and 0.8. These different ratios do not induce significant divergences of relaxivities, saturation magnetization, relaxometric radius or hydrodynamic diameter.

Colloïdal stability of iron oxide nanoparticles is certainly one of the key points for the determination of the optimal [Fe]/[CN] ratio. A typical experimental method to investigate the colloidal stability of the particles is based on the study of the time evolution of the hydrodynamic particle size by Dynamic Light Scattering (DLS) and the influence of the ionic strength [38]. In this work, a relaxometric analysis was performed to control the stabilization of the superparamagnetic particles. Indeed, the aggregation of the nanomagnets has two consequences on the proton relaxation properties: on one hand, those related to the global structure of the cluster and to the magnetic field distribution around them and, on the other hand, those limited to the inner part to the aggregate. While the global effect dominantly causes an increase in the transverse relaxation, the inner one induces a decrease of longitudinal relaxivities. Therefore, the evolution of r_2/r_1 ratios between one and fifteen days after the stabilization is a good indicator of the agglomeration level of superparamagnetic colloïds [39,40]. In this study, only the r_2/r_1 ratio of the cyanoferrofluid characterized by a [Fe]/[CN] = 0.8 increases with time (Fig. 2a). The aggregation phenomenon for this sample can also be confirmed by a rise of hydrodynamic size (d_H = 120 nm, after 15 days).

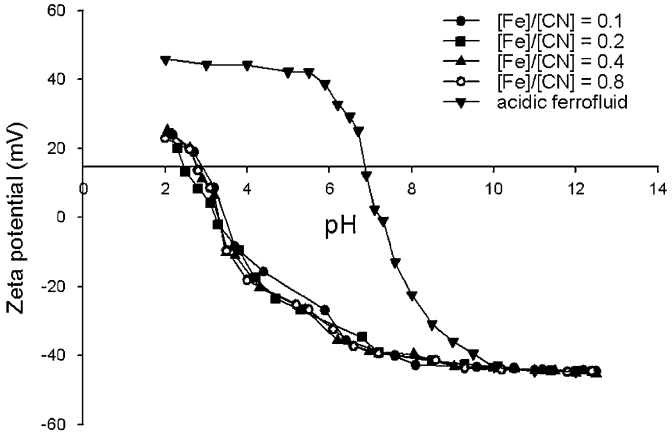

Fig. 1. Evolution of zeta potential of ferrofluids with pH for different [Fe]/[CN] ratios.

Table 1
Physicochemical characteristics of the cationic ferrofluid and of the cyanoferrofluid according to the [Fe]/[CN] ratio.

[Fe]/[CN]	r_1 (s^{-1} mM^{-1})	r_2 (s^{-1} mM^{-1})	r_2/r_1 (20 MHz)	r_2/r_1 (60 MHz)	r_{relaxo} (nm)	$M_{S_{relaxo}}$ ($A.m^2$/kg ferrite)	d_H (nm)
Cationic ferrofluid	49.5	113.1	2.28	5.23	5.7	58.7	25
0.8	54.6	136.7	2.5	5.41	5.8	60.5	29
0.4	55.3	141.6	2.56	5.52	5.8	61	28
0.2	54.5	139.4	2.55	5.61	5.7	60.9	29
0.1	53.1	134.3	2.53	5.48	5.7	61.8	30

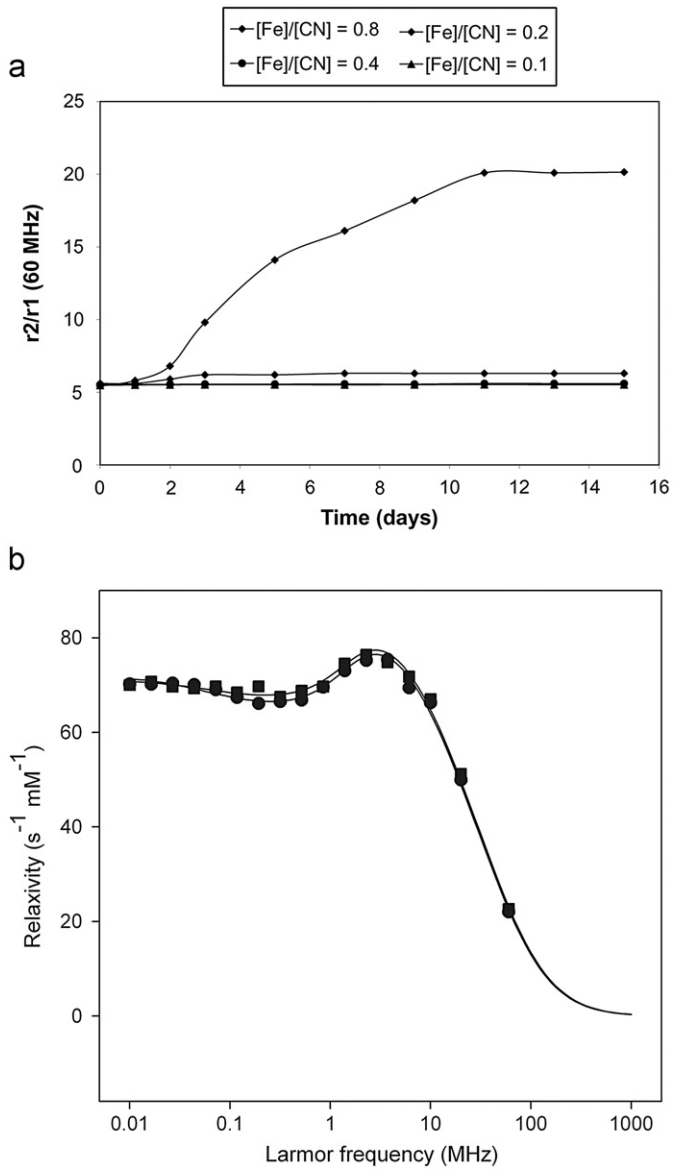

Fig. 2. Evolution of r_2/r_1 ratio according to time (a) and NMRD profiles of cyanoferrofluid ([Fe]/[CN]=0.4) one day and two weeks after the stabilization process (b).

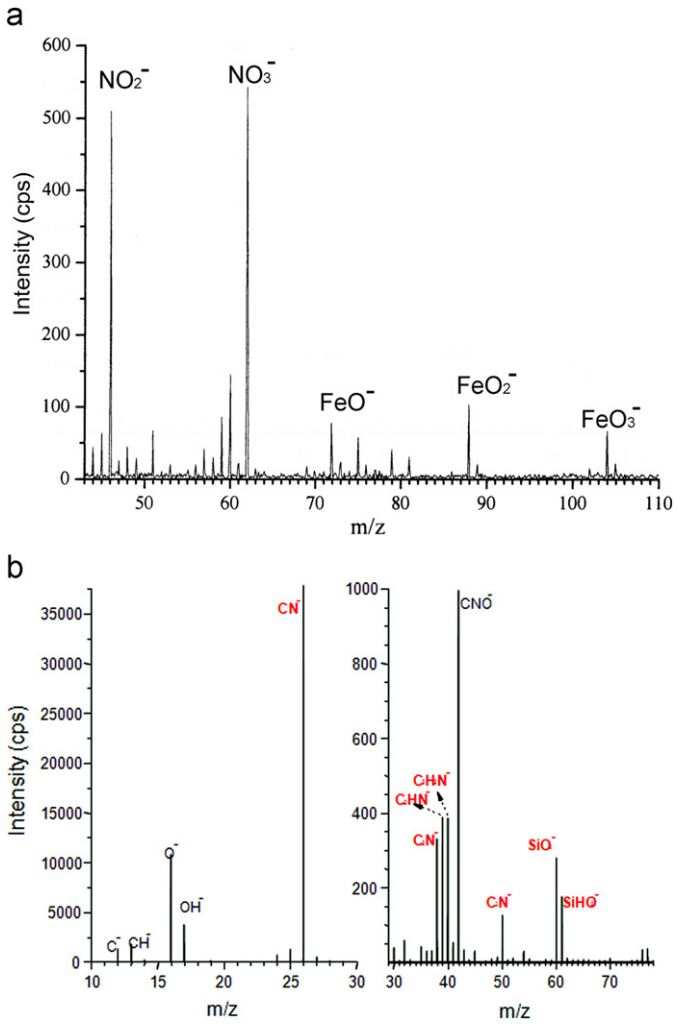

Fig. 3. Negative TOF-SIMS spectra of synthesized magnetite stabilized in acidic conditions (a) and of cyanoferrofluid ([Fe]/[NH_2]=0.4) (b).

If [Fe]/[CN]=0.4, a fast and efficient stabilization can be obtained (d_H=30 nm, after 15 days). The relaxometric profiles are very sensitive to the size dispersion and to particle agglomeration. The colloidal stability of the cyanoferrofluid obtained with [Fe]/[CN]=0.4 is confirmed by the superposition of the relaxometric curves recorded for the same sample one day and 15 days after the synthesis (Fig. 2b).

In order to facilitate the interpretation of these results, a similar stabilization study was carried out with aminopropyltrimethoxysilane (APS). Contrarily to cyanoferrofluid, the zeta potential measurement confirmed previous results in the literature [41], showing an increase of PZC from pH=7 in the magnetite sample to 10.5 after silanization. Moreover, in our stabilization conditions, a higher concentration of APS is necessary ([Fe]/[NH_2]=0.25) to obtain an optimal stability.

In conclusion, this relaxometric and zetametric study allowed us to determine the optimal [Fe]/[CN] ratio (=0.4) to obtain a sufficient density of covering on the iron oxide nanoparticles and a satisfying time stability.

Time of flight secondary ion mass spectrometry (TOF-SIMS) is a powerful characterization tool for obtaining chemical information on the particle surface. Fig. 3a shows the presence of fragments characteristic of the magnetite peptization in acidic conditions before the silanization process (peaks at m/z=46 (NO_2), 62 (NO_3)). From Fig. 3.b, we can confirm the surface modification of the iron oxide particles by CES coating with the principal peaks components at m/z=16 (O), 26 (CN), 42 (CNO), 59.9 (SiO_2), 60.9 (SiOOH) and the disappearance of peaks characteristics of magnetite.

This part of this study allowed defining the optimal stabilization conditions by a coupling agent in order to obtain a new generation of magnetic ferrofluids for biomedical applications. However, the TEM analysis (Fig. 4) shows a relatively broad size distribution, typically log-normal. The presence of several size populations in ferrofluids is often problematic because of the close relationship between the nanoparticles' biomedical efficiency and their physicochemical properties. Thus, a separation method is often necessary to narrow the size distribution.

3.2. Acquisition of a monodisperse cyanoferrofluid

In order to reduce the polydispersity of the ferrofluids, we used a previously described magnetic size sorting procedure [30]. It allows isolating the very small superparamagnetic particles from the larger

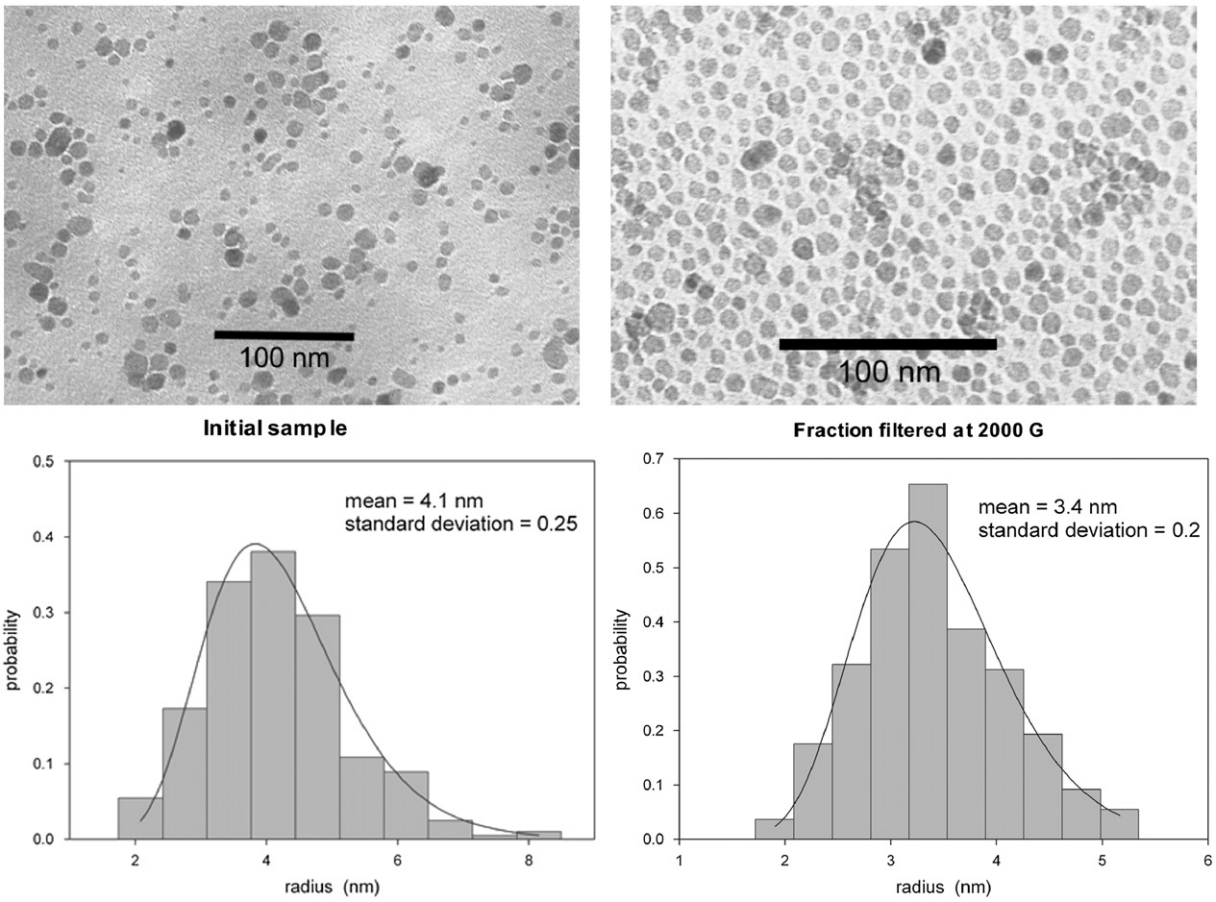

Fig. 4. TEM images and histograms of particle sizes of the initial cyanoferrofluid before and after the magnetic sorting at 2000 G.

Table 2
Physicochemical characteristics of the cyanoferrofluids before and after magnetic sorting at different magnetic fields.

	d_H (nm)	r_2/r_1 (20 MHz)	r_{relaxo} (nm)	$r_{magneto}$ (nm)	PI	Purification yield (%)
Initial sample	28 nm polydisperse	2.56	5.8	5.2	0.1	/
2000 G	14 nm monodisperse	1.71	4.2	4.1	0.024	11.4
1000 G	16 nm monodisperse	1.91	4.9	4.8	0.02	45.3
750 G	16 nm monodisperse	1.99	5.2	5	0.04	49.8
500 G	19 nm polydisperse	2.12	5.4	5.1	0.078	56.8
250 G	20 nm polydisperse	2.27	5.7	5.2	0.096	60.2

ones. The initial cyanoferrofluids were filtered at magnetic fields comprised between 250 G and 2000 G. Table 2 shows the relaxometric and magnetometric properties, the crystal radius and the hydrodynamic size of the initial sample and of the filtered fractions obtained at each field. The difference between these values reflects an evolution of the particles' size distribution during magnetic sorting. For high magnetic fields (2000, 1000 and 750 G), the hydrodynamic size measurement shows the presence of only one population.

The evaluation of the size distribution was also performed by comparing the radius obtained by magnetometry and by relaxometry. The radius obtained by magnetometry is a volume-weighted mean value whereas the one obtained by relaxometry is an intensity-weighted mean value. The equality between the size values would reflect a narrow and unimodal size distribution. Because of its rapidity, the Polydispersity Index (PI, Eq. (3)), based on these measurements, has been proposed and validated previously as an interesting parameter to evaluate the size distribution of each

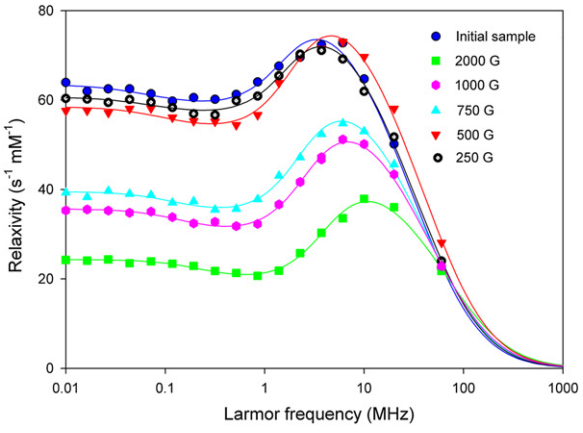

Fig. 5. Comparison of the NMRD profiles of the cyanoferrofluids before and after the magnetic sorting at different magnetic fields.

Table 3
Physicochemical characteristics of the final cyanoferrofluid.

	d_H (nm)	r_1 (s^{-1} mM^{-1}) 20 MHz	r_2 (s^{-1} mM^{-1}) 20 MHz	r_{relaxo} (nm)	$M_{S_{relaxo}}$ (Am^2/kg)	$r_{magneto}$ (nm)	$M_{S_{magneto}}$ (Am^2/kg)	PI
Cyanoferrofluid	16 nm monodisperse	43.6	83.3	4.9	63.5	4.8	66.3	0.02

magnetic fraction.

$$PI = \frac{r_{relaxo} - r_{magneto}}{r_{magneto}} \quad (3)$$

The smaller the PI, the narrower is the size distribution.

A field of 2000 G allows obtaining a monodisperse population of particles with a small PI. The size histograms obtained from TEM (Fig. 4) also show a modification of the distribution shape, passing from a log-normal distribution to a Gaussian distribution (by eliminating the larger particles). A decrease of the mean radius and of the standard deviation σ is observed after the size sorting.

The analysis of the NMRD profiles of the original suspension and of each fraction provides interesting information to evaluate their potential efficiency for MRI. As illustrated in Fig. 5, the relaxivity of the fraction obtained at 2000 G is too low for a biomedical use. On the contrary, for a field ranging between 500 and 250 G, the colloidal dispersion is characterized by an interesting relaxivity but the size sorting seems to become less selective in the retention of large particles (high PI and polydisperse size distribution).

In conclusion, a magnetic field of 1000 G seems optimal to reduce the polydispersity of the particles while keeping interesting relaxivites, a high saturation magnetization, a narrow size distribution (small PI), and a hydrodynamic diameter typical of USPIO (Table 3) with a purification yield of 45.3%.

It is also important to check if magnetic filtration deteriorates the cyanoferrofluid colloidal stability obtained previously. Again, the constant r_2/r_1 evolution with time proves the optimal stabilization of the monodisperse cyanoferrofluid.

4. Conclusions

In this work, a multistep preparation of magnetic ferrofluids was optimized. After the colloïdal magnetite synthesis, the surface of the particles was modified by cyano groups and, finally, their size distribution was narrowed in order to obtain USPIO.

This study allowed determining the optimum conditions for chemical surface modification of magnetite nanoparticles by a silane coupling agent: cyanoethyltrimethoxysilane. The obtained cyanoferrofluid is characterized by different properties such as an interesting transverse relaxivity, a hydrodynamic diameter typical of USPIO and an optimal colloïdal stability at physiological pH. The synthesized particles are thus very good candidates for biomedical applications. Indeed, the presence of cyano groups at the surface of the magnetite opens many perspectives for a further vectorization (click-chemistry) or for *in vitro* cellular labeling studies, thanks to the presence of negative charges at physiological pH.

Acknowledgements

The authors thank Mrs. Patricia de Francisco for her help in preparing the manuscript. The authors also thank Materia Nova for transmission electron microscopy (TEM) studies and for time of flight secondary ion mass spectrometry (TOF-SIMS) analysis. DF is grateful to the FRIA for financial support. Support and sponsorship of the COST Action D38, EMIL NoE program, NOMADE program of the Walloon Region, ARC program of the French Community of Belgium are kindly acknowledged.

References

[1] D.L.J. Thorek, A.K. Chen, J. Czupryna, A. Tsourkas, J. Biomed. Eng. 34 (2006) 23.
[2] A.K. Gupta, C. Berry, M. Gupta, A. Curtis, IEEE Trans. Nanobiosci. 2 (2003) 256.
[3] Q.A. Pankhurst, J. Connolly, S.K. Jones, J. Dobson, J. Phys. D: Appl. Phys. 36 (2003) 167.
[4] E. Duguet, S. Vasseur, S. Mornet, J.M. Devoisselle, Nanomedicine 1 (2006) 157.
[5] B.Y. Xia, B. Gates, Y. Yin, Y. Lu, Adv. Mater. 12 (2000) 693.
[6] B.V. Dejarguin, L. Landau, Acta Physicochim. URSS 14 (1941) 633.
[7] S. Laurent, D. Forge, M. Port, A. Roch, C. Robic, L. Vander Elst, R.N. Muller, Chem. Rev. 108 (2008) 2064.
[8] A.K. Gupta, R.R. Naregalkar, V.K. Vaidya, M. Gupta, Nanomedicine 2 (2007) 23.
[9] A.K. Gupta, M. Gupta, Biomaterials 26 (2005) 3995.
[10] V.I. Shubayev, T.R. Pisanic II, S. Jin, Adv. Drug Delivery Rev. 61 (2009) 467.
[11] M.Mahmoudi, S. Sant, B. Wang, S. Laurent, T. Sen, Adv. Drug Delivery Rev. (2010), 10.1016/j.addr.2010.05.006.
[12] C Corot, P Robert, J.M. Idée, M Port, Adv. Drug Delivery Rev. 58 (2006) 1471.
[13] M. Mahmoudi, A. Simchi, A.S. Milani, P. Stroeve, J. Colloid Interface Sci. 336 (2009) 510.
[14] K.M. Krishnan, IEEE Trans. Magn. 46 (2010) 2523.
[15] A. Petri-Fink, B. Steitz, A. Finka, J. Salaklang, H. Hofmann, Eur. J. Pharm. Biopharm 68 (2008) 129.
[16] M. Ma, Y. Zhang, W. Yu, H.Y. Shen, H.Q. Zhang, N. Gu, Colloids Surf. A: Phys. Eng. Asp. 212 (2003) 219.
[17] R. DePalma, S. Peeters, M.J. Van Bael, H. Van den Rul, K. Bonroy, W. Laureyn, J. Mullens, G. Borghs, G. Maes, Chem. Mater. 19 (2007) 1821.
[18] M. Yamaura, R.L. Camilo, L.C. Sampaio, M.A. Macêdo, M. Nakamura, H.E. Toma, J. Magn. Magn. Mater. 279 (2004) 210.
[19] S. Campelj, D. Makovec, M. Drofenik, J. Magn. Magn. Mater. 321 (2009) 1346.
[20] P.J. Majewski, T.M. Fuchs, S Prakash, Mater. Forum 29 (2005) 489.
[21] S. Falipou, J.M. Chovelon, C. Martelet, J. Margonari, D. Cathignol, Bioconjugate Chem. 10 (1999) 346.
[22] H.C. Kolb, M.G. Finn, K.Barry Sharpless, Angew. Chem. Int. Ed. 40 (2001) 2004.
[23] S. Boutry, S. Brunin, I. Mahieu, S. Laurent, L. Vander Elst, R.N. Muller, Contrast Media Mol. Imaging. 3 (2008) 323.
[24] A.C. Hunter, Adv. Drug Deliv. Rev. 58 (2006) 1523.
[25] I.J. Bruce, T. Sen, Langmuir 21 (2005) 7029.
[26] A.J. Barker, B. Cage, S. Russek, C.R. Stoldt, J. Appl. Phys. 98 (2005) 063528.
[27] A. Del Campo, T. Sen, J.P. Lellouche, I.J. Bruce, J. Magn. Magn. Mater. 293 (2005) 33.
[28] E. Duguet, S. Mornet, J. Portier, brevet FR2855315, 2004.
[29] C.W. Jung, P. Jacobs, Magn. Reson. Imaging 13 (1995) 661.
[30] D Forge, Y Gossuin, A Roch, S Laurent, L Vander Elst, R.N. Muller, Contrast Media Mol. Imaging 5 (2010) 1.
[31] D. Forge, A. Roch, S. Laurent, H. Tellez, Y. Gossuin, F. Renaux, L. Vander Elst, R.N. Muller, J. Phys. Chem. 112 (2008) 19178.
[32] A. Ouakssim, S. Fastrez, A. Roch, S. Laurent, Y. Gossuin, C. Pierart, L. Vander Elst, R.N Muller, J. Magn. Magn. Mater. 272 (2004) 1711.
[33] A Roch, R.N. Muller, P Gillis, J. Chem. Phys. 110 (1999) 5403.
[34] S. Boutry, D. Forge, C. Burtea, I. Mahieu, O. Murariu, S. Laurent, L. Vander Elst, R.N. Muller., Contrast Media Mol. Imaging. 4 (2009) 1.
[35] R Massart, IEEE Trans. Magn. 17 (1981) 1247.
[36] P.J. Majewski, T.M. Fuchs, Adv. Powder Technol. 18 (2007) 303.
[37] Y. Sun, L. Duan, Z. Guo, Y.D. Mu, M. Ma, L. Xu, Y. Zhang, N. Gu, J. Magn. Magn. Mater 285 (2005) 65.
[38] M Schudel, S.H. Behrens, H. Holthoff, J. Colloid Inter. Sci. 196 (1997) 241.
[39] A. Roch, Y. Gossuin, P. Gillis, R.N. Muller., J. Magn. Magn. Mater. 293 (2005) 532.
[40] R.N. Muller, L. Vander Elst, A. Roch, J.A. Peters, E. Csajbok, P. Gillis, Y. Gossuin, Adv Inorg. Chem. 57 (2005) 239.
[41] S. Mornet, J. Portier, E. Duguet, J. Magn. Magn. Mater. 293 (2005) 127.